한국지반공학회논문집 제19권 2호 2003년 4월 pp. 123 ~ 133

The Importance of Geotechnical Variability in the Analysis of Earthquake-induced Slope Deformations

지진으로 인한 사면변위 해석 시 지반성질 모델의 중요성

Kim, Jin-Man* 김 진 만

요 지

사면안정 신뢰성 해석을 통해 다양한 불확실성을 체계적으로 모델링할 수 있는 실용적인 확률통계 기법을 제시한다. 새로운 제안식은, 지반성질의 확률적 특성화를 위해 공간적 변화와 공간평균으로 인한 분산감소뿐만 아니라 통계 및 측정오차까지도 고려하였다. 지진하중의 불확실성은 인공지진파를 대량으로 생성하고 이를 응답해석에 이용함으로써 반영하였다. 예제 해석결과, 한반도와 같이 지진이 활발하지 않은 지역(중약진 지진대)에서는 일반적 수준의 지반성질 변화 특성화가 지진위험도 특성화만큼이나 사면 파괴 위험도와 과도한 사면변형 계산값에 영향을 준다는 결론에 도달하였다.

Abstract

A practical statistical approach that can be used to model various sources of uncertainty systematically is presented in the context of reliability analysis of slope stability. New expressions for probabilistic characterization of soil properties incorporate sampling and measurement errors, as well as spatial variability and its reduced variance due to spatial averaging. The stochastic nature of seismic loading is studied by generating a large series of hazard-compatible artificial motions, and by using them in subsequent response analyses. The analyses indicate that in a seismically less active region such as the Korean Peninsular, a moderate variability in soil properties has an effect as large as the characterization of earthquake hazard on the computed risk of slope failure and excessive slope deformations.

Keywords : Artificial ground motion, Earthquake, Probabilistic analysis, Slope deformation, Spatial variability

1. Introduction

The analysis of seismically induced permanent deformations of slopes involves two basic sources of uncertainty. One source of uncertainty is due to the natural variability of material properties and the uncertainty arising from measurement error and sampling uncertainty. The other major source of uncertainty is the seismic loading itself. Most previous approaches, however, have focused either on material uncertainty or on uncertainty of seismic loading (e.g., Constantinou et al. 1984, Yegian et al. 1991). Thus, it has been difficult to judge the overall impact of uncertainties on the problem, and also their relative significance.

In this paper, we present a practical probabilistic approach that can systematically model various sources of uncertainty found in the assessment of seismically induced permanent deformations of slopes. The stochastic nature of spatially varying material properties and also the uncertainty arising from insufficient information are

* Member, Principal Research Engineer, Hyundai Institute of Construction Technology, jmkim@hdec.co.kr

treated as a random field. The stochastic nature of seismic loading is approached by generating a large series of hazard-compatible artificial motions, and by using them in subsequent response analyses. This approach incorporates probabilistic concepts into the classical limit equilibrium and the Newmark-type (Newmark 1965) deformation techniques. The risk of damage is then computed by reliability-based computational techniques including the Monte Carlo simulation.

The applicability of the proposed approach is illustrated with example seismic slope stability analyses. The results are then interpreted to examine the overall impact of uncertainties on the problem and also their relative significance in seismic slope stability.

2. Spatial Variability

It is well recognized that soil properties vary spatially as a result of depositional and post-depositional processes that cause variation in properties such as mineral composition, moisture content, stress history, and shear strength, etc. In addition, there are a number of other factors, including insufficient sampling and measurement errors, which make it difficult to determine soil properties precisely. In practice, measurements are taken at selected locations and the soil properties, except at the sampling points, are not certain and therefore, may be considered as random quantities. These spatial variations of soil properties can be effectively described by their correlation structure within the framework of random fields (Vanmarcke 1983).

2.1 Statistics of Spatial Averages

Although the continuous variation of the random field is describable, it is seldom useful or necessary to describe in detail the local point-to-point variation. For example, in slope stability analysis we are interested in the statistics of the local average of the material property along the slip surface, since soils generally exhibit plastic behavior and the stability of a soil slope tends to be controlled by the averaged soil strength rather than the soil strength at a particular location along the slip surface. The averaging domain can be a portion of space where a test has been carried out, or a slice of soil mass over which an average property of the material is sought. For the sake of simplicity we will first consider that the data is error free.

The spatially weighted average $\bar{v}$ of a random property $v(\mathbf{x})$ over the element Ω_e can be defined as the stochastic integral:

$$\bar{v} = \frac{1}{V}\int_{\Omega_e} v(\mathbf{x})\,d\mathbf{x} \;\; ; \;\; V = \int_{\Omega_e} d\mathbf{x} \;\; ; \;\; \mathbf{x} \in \Omega_e \qquad (1)$$

where $d\mathbf{x}$ is an elementary volume, area or line element in the three-, two- and one-dimensional cases, respectively.

The covariance of the spatial average $\bar{v}$ between the element domains Ω_e and Ω_e' can then be manipulated in terms of the statistics of point random property $v(\mathbf{x})$ as (Vanmarcke 1983):

$$\begin{aligned}\mathrm{cov}[\bar{v},\bar{v}'] &= E\{[\bar{v} - E(\bar{v})][\bar{v}'-E(\bar{v}')]\} \\ &= \frac{1}{VV'}\int_{\Omega_e}\int_{\Omega_e'} \sigma(\mathbf{x})\sigma(\mathbf{x}')\rho(\mathbf{x},\mathbf{x}')\,d\mathbf{x}d\mathbf{x}' \end{aligned} \qquad (2)$$

where the random property can be described with trend and random components : $v(\mathbf{x}) = \mu(\mathbf{x}) + \varepsilon(\mathbf{x})$.

If the field is second moment (weakly) stationary field, $\sigma(\mathbf{x})\,\sigma(\mathbf{x}')$ and the correlation coefficient $\rho(\mathbf{x}, \mathbf{x}')$ can be replaced by σ^2 and $\rho(\mathbf{r})$ respectively, where $\mathbf{r}$ is a lag distance vector between the $\mathbf{x}$ and $\mathbf{x}'$: $\mathbf{r} = (x_1 - x_1', x_2 - x_2', \ldots, x_n - x_n')$. Then the covariance of the spatial average can further be simplified as:

$$\mathrm{cov}[\bar{v},\bar{v}'] = \sigma^2 \cdot \gamma(\Omega_e, \Omega_e') \qquad (3)$$

where $\gamma(\Omega_e, \Omega_e') = \frac{1}{VV'}\int_{\Omega_e}\int_{\Omega_e'} \rho(\mathbf{r})\,d\mathbf{x}d\mathbf{x}'$.

In the above formulations, $\gamma(\Omega_e, \Omega_e')$ may be called the covariance reduction factor. It should be noted that the reduction factor is dependent only on the correlation function and geometry of the domain of interest and independent of the magnitude of the point variance. The reduction factor is bounded by 0 to 1 since the correlation coefficient is always given equal to or less than unity. Therefore, the variability of local average is always less than that of the point value and further decreases as the size of the averaged domain increases.

2.2 Observation-based Spatial Averages

Uncertainty in the determination of soil properties comes from various sources. One obvious source of uncertainty is the inherent randomness of the natural phenomena (e.g., spatial variation). Other sources of uncertainty include the inaccuracies in the estimation of the parameters and in the choice of the distribution representing the randomness, due to limited observational data, and errors (including random errors and bias) incurred in taking the measurements. Following derivations are based on homogeneous random field. We begin with the unconditional approach that does not account for the location of measurements.

Suppose that $v(\mathbf{x})$ has been observed at N points (or areas) inside and/or around the homogeneous zone of interest. Each observation v_i^* may be associated with a true value v_i and a measurement error e_i. The measurement bias can be modeled by introducing the bias factor B, with mean and variance being denoted as μ_B and σ_B^2 respectively (e.g., Tang 1984, Baecher 1984) :

$$v_i = B_i v_i^* + e_i; \quad i = 1,2,....,N \tag{4}$$

As the true soil properties are unknown, statistics of the soil properties are estimated based on the measured values. Let us assume, for the moment, that the observations are made at sufficiently large distance from each other (statistically independent), e_i has zero mean, a standard deviation σ_e, and lacks autocorrelation and is orthogonal to v^* and v (i.e., the measurement errors are independent each other and independent of observed data). Unbiased sample moments may be used as point estimates of the corresponding moments of population :

$$\mu \approx \hat{\mu} = \frac{1}{N}\sum_{i=1}^{N}[B_i v_i^* + e_i] \tag{5}$$

The above estimates, however, do not convey information on the degree of accuracy of those estimates of parameters, which depends mainly on the number of the observations. The observational data v_i^* can be conceived to be imperfect realizations of a set of independent sample random variables $V_i;\ i = 1, 2, \ldots, N$ among the population and then the sample mean $\hat{\mu}$ can be regarded as a random variable, given as:

$$\hat{\mu} = \frac{1}{N}\sum_{i=1}^{N}[B_i V_i^* + e_i] \tag{6}$$

Its mean value is then given as:

$$E[\hat{\mu}] = \frac{1}{N}\sum_{i=1}^{N}[E(B_i V_i^*) + E(e_i)] = \frac{B}{N}\cdot N\frac{\mu}{B} = \mu \tag{7}$$

and its variance is:

$$\text{var}[\hat{\mu}] = \text{var}\left[\frac{1}{N}\sum_{i=1}^{N}(B_i V_i^* + e_i)\right] \approx \frac{\mu_B^2\sigma^{*2} + \mu^{*2}\sigma_B^2 + \sigma_B^2\sigma^{*2} + \sigma_e^2}{N} \tag{8}$$

When there is no bias ($\mu_B = 1$ and $\sigma_B^2 = 0$), the sample mean $\hat{\mu}$ has a standard deviation (or error) $(\sigma^* + \sigma_e)/\sqrt{N}$.

Now, first two moments of spatial average can be estimated based on the observational data, taking account of not only point estimates but also degree of accuracy of those estimations.

The expected value of the spatial average can be evaluated by replacing μ with sample mean $\hat{\mu}$ as:

$$E[\overline{v}] = E\left[\frac{1}{V}\int_{\Omega_e}(\hat{\mu} + \varepsilon(\mathbf{x}))\, d\mathbf{x}\right] = E[\hat{\mu} + \varepsilon(\mathbf{x})] = \mu \tag{9}$$

Similarly, the covariance between two spatial averages is given (Kim 2001):

$$\text{cov}[\overline{v},\overline{v}'] \approx \frac{\mu_B^2\sigma^{*2} + \mu^{*2}\sigma_B^2 + \sigma_B^2\sigma^{*2} + \sigma_e^2}{N} + \sigma^2\gamma(\Omega_e,\Omega_e') \tag{10}$$

The first term in the above solution (Equation 10) represents sampling and measurement errors (i.e., uncertainties in the estimation of the sample mean) while the second term is the reduced variance due to the spatial average. Figure 1 shows the comparison of magnitude of

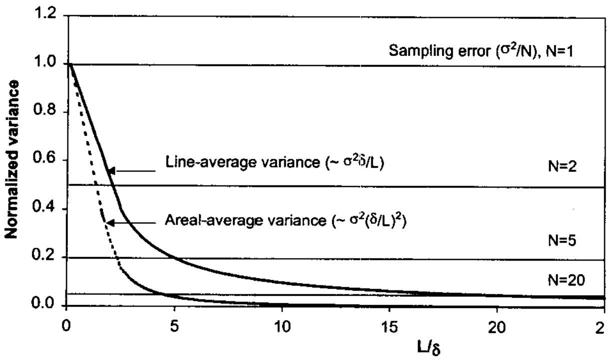

Fig. 1. Comparison of the uncertainty magnitudes between the spatial variation (inherent uncertainty) and sampling error (statistical uncertainty); N is the number of tests, L is the sale of averaging, and δ is the sale of fluctuation

uncertainty between the spatial variation and sampling error. Unlike the inherent uncertainty, errors from the insufficient data and imperfect measurement do not decrease by averaging over the area of space, but depend on the number of samples. In the special case of var($\hat{\mu}$)=0, which happens when $N\rightarrow\infty$, the above solution (Equation 10) becomes identical with Equation 3.

Tang (1984) reported a relationship which is similar to Equation 10. His formula, however, is based on the first order approximation of various sources of uncertainties that are factored and therefore may not be applicable to a problem with sources of large uncertainty (Kim and Sitar *in review*). Li and White (1987) reported similar relationships to Equation 10, although their formulas do not include the measurement error and bias terms as presented herein.

An important and highly desirable characteristic of a random field simulation is that the random field simulation reproduces the observed values at their respective sampling locations. Conditional simulation, or ordinary kriging (OK), has this very desirable property and it has been extensively used in many different applications, particularly mineral exploration (see e.g. Krige 1966, Journel 1989).

When prior estimate of the mean value of a property is not available, as is usually the case in most field exploration problems, a linear estimator may be expressed in a weighted linear combination of the observed values in the form:

$$\hat{v}_a = \hat{v}(\mathbf{x}_a) = \sum_{j=1}^{N} w_{aj} v_j = \sum_{j=1}^{N} w_{aj}(B_j v_j^* + e_j) \tag{11}$$

Requirements that the estimator be unbiased and the expected value of its squared error be minimal yield the following conditions for weights w_{aj}:

$$\sum_{j=1}^{N} w_{aj} = 1 \tag{12}$$

$$\sum_{j=1}^{N} w_{aj}\sigma^*_{jk} - \lambda_a = \sigma^*_{ak};\ \ k = 1, \ldots, N \tag{13}$$

where λ_a is a Lagrange multiplier and the asterisk (*) is used to emphasize the fact that the covariance is obtained by including the effects of measurement errors and bias, if any. The above two equations are a system of N+1 linear equations with N unknowns w_{aj} and λ_a. The covariance between two values $\hat{v}_a$ and $\hat{v}_b$ is then given by:

$$\sigma_{OK,ab} = E[(\hat{v}_a - v_a)(\hat{v}_b - v_b)] = \sigma_{ab} - \sum_{k=1}^{N} w_{ak}\sigma^*_{kb} + \lambda_a \tag{14}$$

alternatively,

$$\sigma_{OK,ab} = E[(\hat{v}_a - v_a)(\hat{v}_b - v_b)] = \sigma_{ab} - \sum_{k=1}^{N} w_{bk}\sigma^*_{ka} + \lambda_b \tag{15}$$

The second term in the above expression (Equation 14) represents the reduction in the covariance of the estimator from the ensemble (or point) variance as a result of spatial correlation. If all the observations points and the point to be estimated are separated far enough ($\sigma^*_{ja} \approx 0$; $\sigma^*_{ij} \approx 0$ *for* $i \neq j$,) the estimate may equal to the arithmetic mean, and the ordinary kriging covariance may reduce to:

$$\sigma_{OK,ab} \approx \sigma_{ab} + \lambda_a \approx \sigma^2\gamma(\Omega_a, \Omega_b) + \frac{\mu_B^2\sigma^{*2} + \mu^{*2}\sigma_B^2 + \sigma_B^2\sigma^{*2} + \sigma_e^2}{N} \tag{16}$$

, because $w_{aj}\sigma^*_{jj} = w_{aj}$ var $[v_j] \approx w_{aj}(\mu_B^2\sigma^{*2} + \mu^{*2}\sigma_B^2 + \sigma_B^2\sigma^{*2} + \sigma_e^2 \approx \lambda_a$; $w_{aj} \approx \frac{1}{N}$ from Equations 12 and 13.

It should be noted that uncertainties arising from the sampling and measurement errors are implicitly included in Equation 14, because the mean value needs to be estimated based on observations. Also, Equation 16 is identical to Equation 10 (based on the unconditional evaluation) as they should be.

3. Temporal Variability

In general, ground motions that correspond to a limited number of design parameters are not unique. Consequently, a broad range of responses can be obtained even with a set of motions that match the same target parameters. There have been, in general, three main methods for generation of artificial ground motion: (1) modification of recorded ground motions (e.g., Lilhanand and Tseng 1988); (2) generation of genuine artificial motion in terms of stochastic processes (e.g., Gasparini and Vanmarcke 1976); and (3) generation of artificial motion using Green's function techniques (e.g., Hartzell 1978).

Majority of the procedures developed for generating earthquake ground motions as random (or stochastic) processes are either based on ARMA models (e.g., Shamaras et al. 1985) or spectral representation (e.g., Housner and Jennings 1964). Spectral representation of ground motion with the power spectral density (PSD) function, in general, provides both clear interpretation and computational efficiency. It can also easily incorporate the non-stationarity of the intensity and frequency content.

A periodic function can be expressed by series of sinusoidal motions and, especially, the zero-mean process can be represented as (Rice 1954):

$$X(t) = \sum_{i=1}^{n} \sqrt{2G(\omega_i)\Delta\omega}\, \sin(\omega_i t + \theta_i) \qquad (17)$$

where we adopts the widely quoted form for the PSD function $G(\omega)$ that is based on Kanai (1957) and Tajimi (1960)'s studies. Each different array of phase angles can be modeled by statistically independent random phase angles θ_i, which are uniformly distributed between 0 and 2π. The above formula defines an infinite ensemble of time histories with the same frequency content but with randomly distributed phase angles between the individual components. Sample earthquake motion can then be obtained by directly transforming them into the time domain by *FFT* (*Fast Fourier Transform*, Cooley and Tukey 1965).

Transient character of the intensity content of the earthquake motion can be added by multiplying the stationary motion by a deterministic modulating (envelope) function $m(t)$. The non-stationary motion $Y(t)$ then becomes

$$Y(t) = m(t)X(t) = m(t)\sum_{j=1}^{n} \sqrt{2G\,(\omega_j)\Delta\omega}\, \sin(\omega_j t + \theta_j) \qquad (18)$$

In their liquefaction-related analytical approaches, Wang and Kavazanjian (1987) proposed a trigonometric modulating function that has two model parameters to define the shape of the modulating function, defined as:

$$m(t) = \sin^{\alpha}\left(\pi (t / t_d)^{\beta}\right) \qquad (19)$$

where α and β are two parameters to determine the shape of the modulating function and t_d is the duration of motion. Unlike the conventional models, this model provides a convenient way in developing the statistics of shape parameters since it is in a normalized form and can thus be used independent of the intensity and the duration of the ground motion.

There are different methods for characterizing the temporal variation of the spectral content of earthquake motion. Simple, yet efficient, approach is to divide the ground motion into several sections small enough so that stationarity of the frequency content within each section can be assumed without much error (Saragoni and Hart 1974).

3.1 Relationship between the Modulating Function and RMS Hazard

One of the energy-based parameters is the RMS (Root Mean Square) acceleration, which is defined as (Housner 1975):

$$RMS_a = \sqrt{\frac{E(T_d)}{T_d}} = \left[\frac{1}{T_d}\int_{t_0}^{t_0+T_d} a^2(\tau)d\tau\right]^{1/2} \tag{20}$$

where $a(\tau)$ is acceleration time history, t_0 is initial time of interest, T_d is duration of the strong ground shaking, and $E(T_d)$ is a total energy for the duration T_d. Similarly, temporal RMS can be defined by replacing T_d with a small time interval Δt as:

$$RMS_a(t) = \left[\frac{1}{\Delta t}\int_{t}^{t+\Delta t} a^2(\tau)d\tau\right]^{1/2} \quad for\ \Delta t \to 0 \tag{21}$$

We can define the normalized PSD by dividing the PSD with its variance as:

$$G^*(\omega) = \frac{1}{\sigma^2}G(\omega) \tag{22}$$

When the stationary process $X^*(t)$ is a normalized process with unit variance and PSD function $G^*(\omega)$, equation 18 (non-stationary ground motion) can be rewritten in terms of the normalized PSD function and modulating function $m(t)$ as:

$$Y(t) = m(t)X^*(t) = m(t)\sum_{i=1}^{n}\sqrt{2G^*(\omega_i)\Delta\omega}\sin(\omega_i t + \theta_i) \tag{23}$$

It is fairly straightforward to relate time-variant RMS to the deterministic modulating function $m(t)$ as follows:

$$RMS_Y^2(t) = E\lfloor Y^2(t)\rfloor = m^2(t)E\lfloor X^{*2}(t)\rfloor = m^2(t) \tag{24}$$

The time-variant RMS of the motion $Y(t)$ can thus be identical to the modulating function $m(t)$. In other words, if the normalized power spectral functions are given, non-stationary ground motion can be obtained by a product of the temporal-variant RMS (or time dependent standard deviation) and normalized stationary process of PSD $G^*(\omega)$.

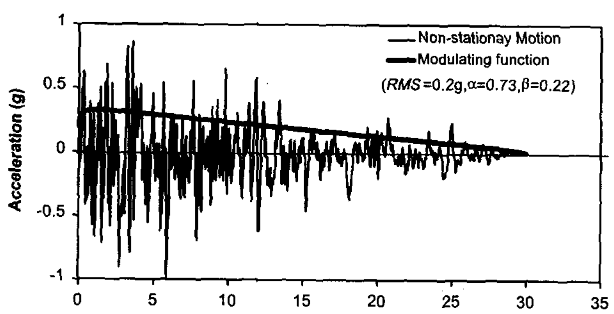

Fig. 2. Sample time history of non-stationary ground motion (RMS=0.2 g, α=0.73, β=0.22, t_d=30 sec)

Figure 2 shows sample earthquake motion generated by using the aforementioned procedures.

4. Limit State Function and Probability of Failure

Conceptually, the performance of a structure can be described by a limit state function (also often called performance function) $g(\mathbf{x})$ so that failure is defined whenever the condition of $g(\mathbf{x}) \leq 0$ is satisfied, where $\mathbf{x}$ is the vector of model variables (Figure 3). The probability of failure is then given by:

$$p_f = P(g(\mathbf{x}) \le 0) = \int_{g(\mathbf{x})\le 0} f(\mathbf{x})d\mathbf{x} \tag{25}$$

where $f(\mathbf{x})$ is the joint probability density function (PDF) of $\mathbf{x}$.

Once the limit state function $g(\mathbf{x})$ and the distribution $f(\mathbf{x})$ are selected, the probability of failure p_f can be estimated by computing the volume of the joint distribution $f(\mathbf{x})$ within the failure domain defined by $g(\mathbf{x}) \leq 0$. During the last four decades, a number of computational methods have been developed to solve efficiently the

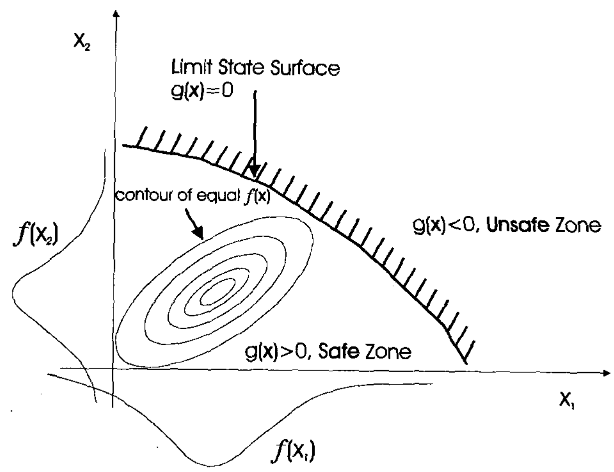

Fig. 3. Limit-state and probability density functions

problem. These include the mean-value first order second moment (MVFOSM or often simply FOSM) (Cornell 1969) and the first- and second-order reliability methods (FORM and SORM) (Madsen et al. 1986). A variety of other computation methods, including simulation methods (Rubinstein 1981) and response surface methods (Faravelli 1989) are also available.

A limit-state function representing the slope deformation under the stochastic seismic loadings is not sufficiently smooth to be differentiable (Kim 2001). When the limit-state functions are not differentiable, those methods (e.g., FOSM, FORM, and SORM) that require the computation of derivatives or gradients of the limit state functions cannot be used, and Monte Carlo simulations provide the alternative.

5. Example Analyses

The purpose of example analyses is to illustrate the influence of various assumptions on the estimated soil properties, earthquake motions, and the resulting probabilities of failure. We are interested in evaluating the risk of failure of a cohesive slope shown in Figure 4. Three vertical borings are carried out and 10 soil samples are taken at the specific locations shown in Figure 4. Subsequent tests yield a sample mean $\bar{c} = 45\ kN/m^2$ and a sample standard deviation $s_c = 13.5\ kN/m^2$ for undrained shear strength, and $\bar{\gamma} = 18\ kN/m^3$ and $s_\gamma = 0.9\ kN/m^3$ for soil density. Previous experience with local geology indicates that the soil can be modeled as a homogeneous random field and the scales of fluctuation may be assumed as $\delta_x = 5m$ and $\delta_y = 1m$ respectively. A separable 2-D exponential autocorrelation function is employed to model the correlation. In addition to the shear strengths, we assume that the shear wave velocity measured at the site ranges from 150 to 250 m/sec. The failure surface

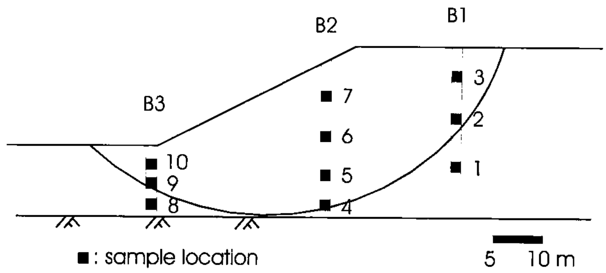

Fig. 4. Geometry and sample location of a slope with a circular slip surface

is considered to be deterministic as it may be in post-failure analyses, although this is simply a convenience and not requirement of our method of solution. The potential sliding mass is divided into 40 vertical soil slices of equal width for subsequent static stability and seismic deformation analyses using Newmark-type deformation techniques (Newmark 1965). Deterministic analyses of the static slope stability, with the mean soil properties, yielded a factor of safety 1.52. Analyses with more adverse soil properties ($\mu - \sigma$ for the shear strengths and $\mu + \sigma$ for soil density) resulted in a factor of safety 1.02.

For the purpose of seismic analyses, the site is assumed to be in Berkeley, California, in the seismically active San Francisco Bay Area. The Hayward fault that is the closest major fault to the site of interest is considered. The computed RMS hazards are de-aggregated into several intervals of intensity, magnitude, and distance. In order to generate RMS-compatible ground motion, we need to specify the frequency content and duration in addition to the RMS acceleration. We adopt the stochastic ground motion parameters, which were suggested by Wang and Kavazanjian (1987) and updated by Tung et al. (1992). Tables 1 and 2 summarize stochastic ground motion parameters selected in this study. Another strong ground motion parameter, which is important in the nonlinear deformation analyses, is duration. The hazard compatible duration can be assigned to each generated

Table 1. Power spectral density parameters for rock sites (from Tung et al. 1992)

Parameter	Distribution	Segment 1		Segment 2		Segment 3	
		μ	σ	μ	σ	μ	σ
ω_g	Gamma	23.57	3.46	21.12	3.60	18.38	3.50
ζ_g	Gamma	0.352	0.360	0.394	0.380	0.417	0.162

Table 2. Parameters for modulating function (from Wang and Kavazanjian 1987)

Parameter	Distribution	μ	σ
α	Rayleigh	0.73	0.45
β	Exponential	0.22	0.18

Table 3. Significant Duration (5-95 % RMS Duration), estimated based on the empirical relationship reported by Abrahamson and Silva (1996)

Magnitude	Distance (kilometers)	Significant Duration (seconds)
5.0-6.0	0-10	3.80
	10-20	4.53
	20-30	6.00
	30-50	8.20
	50-100	13.33
6.0-7.0	0-10	9.05
	10-20	9.78
	20-30	11.25
	30-50	13.45
	50-100	18.58
7.0-7.5	0-10	17.34
	10-20	18.08
	20-30	19.54
	30-50	21.74
	50-100	26.87
7.5-8.0	0-10	26.76
	10-20	27.49
	20-30	28.96
	30-50	31.16
	50-100	36.29

ground motion by means of de-aggregation of total hazard into appropriate intervals of earthquake magnitude and distance to site. Table 3 shows the significant duration (5-95 % Arias duration or 5-95 % RMS duration), which is estimated using the empirical relationship proposed by Abrahamson and Silva (1996).

The slope is assumed to be able to tolerate up to 200 mm of permanent displacement. The limit state function (as explained previously in chapter 4) is thus defined as:

$$g(\mathbf{X}) = 200 - d(\mathbf{X})$$

where d is the permanent deformation of the slope subject to a hazard compatible ground motion. Simulation-based (Monte Carlo) reliability analyses are performed by generating a series of hazard compatible outcrop rock motions, and by using them directly in subsequent slope deformation analyses. In addition to the motions, the

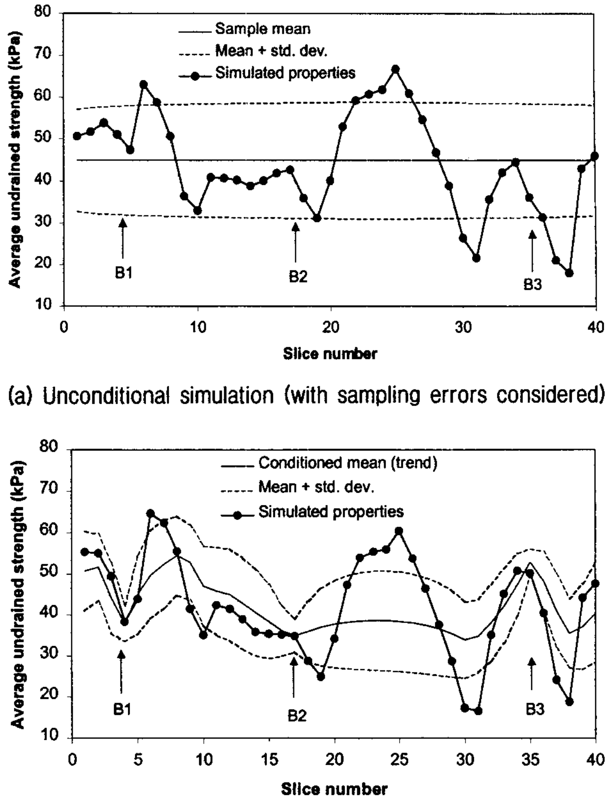

(b) Conditional simulation

Fig. 5. Simulation of average undrained shear strengths

slice-based random soil properties are also generated (Figure 5), and are used as input values to compute the yield acceleration. The numerical implementation and data flow of the probabilistic approach are illustrated in Figure 6.

The computations were carried out with the soil properties modeled with various approaches including conditional (Kriging), unconditional and deterministic

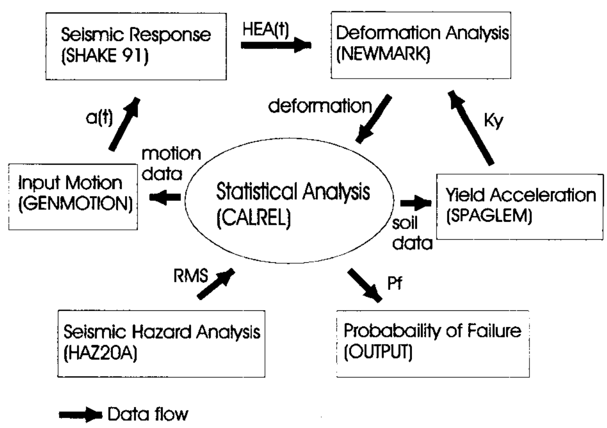

Fig. 6. Numerical implementation and data flow of probabilistic seismic slope deformation analysis

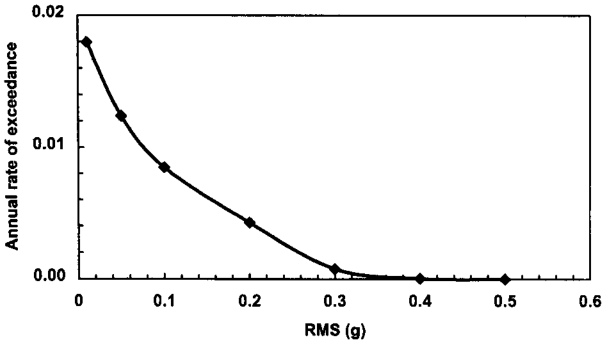

(a) Annual hazard curve (annual rate of exceeding each hazard level)

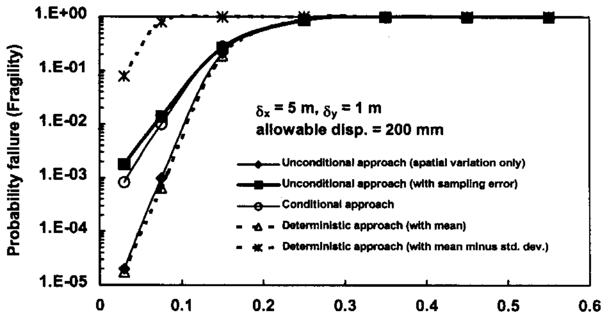

(b) Fragility curve

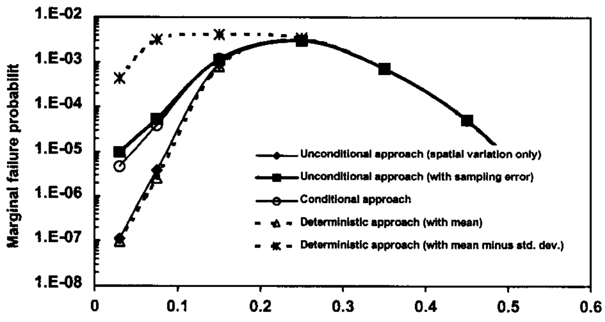

(c) Marginal annual risk curve (annual probability of failure with respect to each hazard level)

Fig. 7

methods in order to examine the influence of different soil property characterizations on the risk level of the problem. Figure 7 shows the computed seismic hazards (often called *hazard curve*), the probabilities of failure given the certain hazard levels (often called *fragility curve*), and the annual probability of exceeding 200 mm displacement (often called *risk curve*) for five different characterizations of soil properties. The seismic hazards are same for the five cases. The difference is the level of uncertainty in soil property determination. The deterministic soil properties represent the lowest level of uncertainty in the property determination, the conditional and unconditional (with sampling error) the highest level of uncertainty, and the unconditional case (spatial variation only) in between these levels. It is interesting to observe that differences in the probabilities of failure for the different cases are significant at the lower level of hazard (< 0.1 g) and gradually decrease with increasing hazard level, being negligible at the higher level (> 0.2 g) except for the case of the mean minus one standard deviation. The case of deterministic mean soil properties provides the lower bound of the risk and the mean minus standard deviation yields the upper bound. Note that the difference between the unconditional (spatial variation only) and the deterministic mean is minimal. That is because of significant variance reduction due to spatial averaging. However, the risk level significantly increases once the sampling error is included. For relatively small correlation lengths ($\delta_x = 5m$ and $\delta_y = 1m$), the difference between the conditional and unconditional (with sampling error) approaches is minimal. Increasing correlation (i.e., increasing δ) yielded a similar trend, but the risk level for the unconditional approaches become higher due to small variance reduction. Additional computation with increased allowable displacement showed essentially the same trends as the original allowable displacement (d = 200 mm), except the risk of failure is lower, as would be expected. Analyses with a high landfill slope yield comparable results (Kim 2001). Thus, the uncertainty of soil properties can have a significant impact on the computed risk of slope failure at relatively low levels of seismic hazard, but it may have a little impact on the computed risk if the slope is exposed to relatively high levels of hazard. In this particular problem, the uncertainty of soil properties arising from the spatial variation and sampling errors has much impact on the reliability of the slope for the RMS hazard level lower than 0.2 g.

6. Conclusions

The results of analyses show that the variability of the local average is always less than that of the point value and that it decreases with the increase of the size of the average domain.

Unlike the inherent uncertainty, errors from the insufficient data and imperfect measurement do not decrease by averaging over the area or space, but depend only on the number of samples. In this context, increasing the sub-domain size is only locally effective in variance reduction and the effect of the total cumulative variance reduction on the risk of the slope failure is the same regardless of the sub-domain size.

The results of analyses show that the conditional approach takes full advantage of the available data and it leads to a more complete understanding of the degree of risk.

Finally, one of the most important findings in this study is that the uncertainty of soil properties can have a significant impact on the computed risk of failure for a slope with spatially correlated soil properties exposed to relatively low levels of seismic hazard (RMS < 0.1 ~ 0.2 g), but it may have a little impact on the computed risk if the slope is exposed to relatively high levels of hazard (RMS > 0.1 ~ 0.2 g). Thus, the results suggest that in a seismically less active region the like Korean Peninsular, a moderate variability in soil properties has an effect as large as the characterization of earthquake hazard on the computed risk of slope failure and the risk of excessive slope deformations.

Acknowledgements

This research was supported in part by the Hyundai Engineering & Construction Co., Ltd. and by Chancellor's Chair funding from the University of California, Berkeley. The author thanks professor Sitar of University of California at Berkeley for reviewing the manuscript.

References

1. Abrahamson, N. and Silva, W. (1996), "Empirical ground motion models, draft Report", Brookhaven National Laboratory.
2. Baecher, G. B. (1984), "Just a few more tests and we'll be sure!", *Proceedings of the Symposium on Probabilistic Characterization of Soil Properties*, Atlanta, Georgia, pp.1-18.
3. Constantinou, M. C., Gazetas, G. and Tadjbakhsh, I. (1984), "Stochastic seismic sliding of rigid mass supported through non-symmetric friction", *Earthquake Engineering and Structural Dynamics*, 12, pp.777-793.
4. Cooley, J. W. and Tukey, J. W. (1965), "An algorithm for the machine calculation of complex Fourier series", *Mathematics of Computation*, 19, pp.297-301.
5. Cornell, C. A. (1969), "Structural safety specification based on second-moment reliability", *Symposium, International Association of Bridge and Structural Engineers*, London.
6. Faravelli, L. (1989), "Response surface approach for reliability analysis", *Journal of Engineering Mechanics*, ASCE, 115(12), pp.2763-2781.
7. Gasparini, D. A. and Vanmarcke, E. H. (1976), "Evaluation of seismic safety of buildings Report No. 2: Simulated earthquake motions compatible with prescribed response spectra", Publication No.R76-4, Department of Civil Engineering, Massachusetts Institute of Technology, Cambridge, Massachusetts.
8. Hartzell, S. (1978), "Earthquake aftershocks as Green's functions", *Geophysical Research Letters*, 5(1), pp.1-4.
9. Housner, G. W. (1975), "Measures of severity of earthquake ground shaking", *Proceedings U.S. National Conference on Earthquake Engineering*, Ann Arbor, Michigan.
10. Housner, G. W. and Jennings, P. C. (1964), "Generation of artificial earthquakes", *Journal of Engineering Mechanics*, ASCE, 90(EM1), pp.113-150.
11. Journel, A. G. (1989), Fundamentals of geostatistics in five lessons, American Geophysical Union.
12. Journel, A. G. and Hujibregts, C. (1978), Mining geostatistics, Academic Press.
13. Kanai, K. (1957), "Semi-empirical formula for the seismic characteristics of the ground", *Bulletin of the Earthquake Research Institute*, Tokyo University, 35, pp.308-325.
14. Kim, J. (2001), "Probabilistic approach to evaluation of earthquake-induced permanent deformation of slopes", Ph.D. Dissertation, Dept. of Civil and Env. Engineering, University of California, Berkeley.
15. Kim, J. and Sitar, N., "Reliability analysis of slope stability with spatially correlated soil properties", *Journal of Geotechnical and Geoenvironmental Engineering*, (submitted for publication).
16. Krige, D. G. (1966), "Two-dimensional weighted moving averaging trend surfaces for ore evaluation", *Proceedings of Symposium on Mathematical Statistics and Computer Applications for Ore Evaluation*, Johannesburg, S. A., pp.13-38.
17. Li, K. S. and White, W. (1987), "Probabilistic characterization of soil profiles", Research Report No.19, Department of Civil Engineering, University College, The University of New South Wales, Canberra, Australia.
18. Lilhanand, K. and Tseng, W. S. (1988), "Development and application of realistic earthquake time histories compatible with multiple damping response spectra", *Ninth World Conference, Earthquake Engineering*, Tokyo, Japan, pp.819-824.
19. Madsen, H. O., Krenk, S. and Lind, N. C. (1986), "Methods of structural safety", Prentice-Hall, Englewood Cliffs, NJ.
20. Newmark, N. M. (1965), "Effects of earthquakes on dams and embankments", *Geotechnique*, 15(2), pp.139-160.
21. Rice, S. O. (1954), "Mathematical analysis of random noise", Selected papers on noise and stochastic processes, N. Wax, ed.,

Dover Publications, New York, pp.133-294.
22. Rubinstein, R. Y. (1981), Simulation and the Monte Carlo method, John Wiley & Sons, New York.
23. Saragoni, G. R. and Hart, G. C. (1974), "Simulation of artificial earthquakes", *Earthquake Engineering and Structural Dynamics*, 2, pp.249-267.
24. Shamaras, E., Shinozuka, M., and Tsurui, A. (1985), "ARMA representation of random processes", *Journal of Engineering Mechanics*, ASCE, 111(3), pp.449-461.
25. Tang, W. H. (1984), "Principles of probabilistic characterization of soil properties", *Proceedings of the Symposium on Probabilistic Characterization of Soil Properties*, Atlanta, Georgia, pp.74-89.
26. Tajimi, H. (1960), "A statistical method of determining the maximum response of a building structure during an earthquake", *Proceedings of the Second World Conference on Earthquake Engineering*, Tokyo, pp.781-797.
27. Tung, A. T. Y., Kiremidjian, A. S., Wang, J. N. and Kavazanjian, J., E. (1992), "Statistical parameters of AM and PSD functions for the generation of site-specific strong ground motions", *Earthquake Engineering, Tenth World Conference.*
28. Vanmarcke, E. (1983). Random fields: analysis and synthesis, The MIT Press, Cambridge, Massachusetts.
29. Wang, J. N. and Kavazanjian, J., E. (1987), "A nonstationary probabilistic model for pore pressure development and site response due to seismic excitation", Report No. 84, The John A. Blume Earthquake Engineering Center, Stanford University.
30. Yegian, M. K., Marciano, E. A. and Ghahraman, V. G. (1991), "Earthquake-induced permanent deformations - Probabilistic approach", *Journal of Geotechnical Engineering*, ASCE, 117(1), pp.35-50.

(received on Nov. 6, 2002, accepted on Apr. 10, 2003)